J Mater Sci: Mater Med (2010) 21:1511–1519
DOI 10.1007/s10856-010-4026-4

Preparation and properties of gold nanoparticle-electrodeposited titanium substrates with Arg-Gly-Asp-Cys peptides

Hui-An Weng · Ching-Chou Wu · Chun-Cheng Chen · Chia-Che Ho · Shinn-Jyh Ding

Received: 29 October 2009 / Accepted: 1 February 2010 / Published online: 17 February 2010

Abstract Titanium metal has good biocompatibility, superior mechanical properties and excellent corrosion resistance. Like most metals, however, it exhibits poor bioactive properties and fails to bond to bone tissue. To improve its bioactivity, bioactive molecules, such as peptides, can be grafted onto titanium surfaces. In order to do this, the first step may be to establish a stable and compatible linking layer on the titanium surface. In this study, we used electrochemical methods to deposit gold (Au) nanoparticles onto titanium substrates, to which we then grafted arginine-glycine-asparagine-cysteine (RGDC) peptides by thiolate covalent coupling. Properties of electrodeposited Au nanoparticles were evaluated using a variety of techniques, including microstructural, chemical and electrochemical measurements. The biological responses of the RGDC-grafted Ti substrates were evaluated using MG3 human osteoblast-like cells. The results of thin-film X-ray diffraction (TFXRD) and scanning electron microscopy (SEM) indicated the polycrystalline orientation of Au nanoparticles deposited on the titanium surfaces with high density and controllable particle size. The RGDC peptide could be covalently bonded to Au-deposited Ti substrates via Au-thiolate species, as expected. Cell morphology showed that, on RGDC-immobilized titanium with Au particles, MG63 cells attached and spread more rapidly than on Ti substrates either without peptide or with direct loading of the peptide. Immunostaining for focal adhesion kinase (FAK) demonstrated that RGDC enhanced cell attachment. The present method for the formation of Au nanoparticles may serve as an alternative route for bioactive molecule immobilization on Ti implants.

H.-A. Weng
Dental Department, Changhua Christian Hospital, 500 Changhua County, Taiwan

C.-C. Wu
Department of Bio-Industrial Mechatronics Engineering, National Chung-Hsing University, 402 Taichung, Taiwan

C.-C. Chen · S.-J. Ding
Department of Dentistry, Chung-Shan Medical University Hospital, 402 Taichung, Taiwan

C.-C. Chen · S.-J. Ding
School of Dentistry, Chung-Shan Medical University, 402 Taichung, Taiwan

C.-C. Ho · S.-J. Ding (✉)
Institute of Oral Biology and Biomaterials Science, Chung-Shan Medical University, No. 110, Sec. 1, Jinguo North Road, 402 Taichung, Taiwan
e-mail: sjding@csmu.edu.tw

1 Introduction

Over the past few decades, considerable effort has been devoted to the development of surgical implant metals for load-bearing prosthetics. Metals like titanium, cobalt-chromium alloys and stainless steel have been the focus of most investigations because they have superior mechanical properties. The most promising materials are titanium and titanium alloys because of their excellent biocompatibility and higher resistance to corrosion [1]. However, like most metals, titanium has poor bioactive properties and fails to bond to bone tissue [1–3]. Many researchers have attempted to improve the bioactivity of titanium surfaces by creating bioceramic coatings or by modifying the implant surface [3–10]. For example, Nagai et al. [7] showed that coating titanium implants with collagen enhanced the attachment of

peri-implant soft tissue to the titanium shortly after implantation. The immobilization of bioadhesive molecules, such as peptides, proteins or growth factors, on titanium surfaces via covalent bonding is another strategy for the purpose of inducing specific cell responses [10–17]. Nanci et al. [10] functionalized oxidized titanium surfaces with covalently bonded biomolecules, such as alkaline phosphatase or albumin, using an intermediary aminoalkylsilane. A short chain peptide commonly present in the extracellular matrix, such as the Arg-Gly-Asp (RGD) peptide, is able to promote cell attachment, proliferation and differentiation. Xiao et al. [13] applied a three-step reaction procedure, including pretreatment, silanization and cross-linking, to introduce RGD-containing peptides onto a titanium surface.

Gold has been widely used in many applications because of its biocompatibility and other specific properties. Studies have reported that thiol (–SH) groups could be grafted onto gold surfaces via a strong covalent linkage [18], through which the immobilization of a biomolecular layer can be carried out. Nano-sized gold metals have specific optical, physical, chemical and superior catalytic properties, as well as relatively high surface area-to-volume ratios compared to their bulk material. Several methods have been developed for the fabrication of nano-sized gold particles, such as chemical reduction [19], deposition–precipitation [20] and electrochemical deposition [21]. Among these techniques, electrochemical deposition is a promising technique for preparing nanoparticles due to its ease of use and low cost of implementation. Li et al. [22] improved the sensitivity of DNA-binding drug impedance sensors by electrodepositing gold nanoparticles on Au electrodes.

The classical immobilization schemes for biomolecules on titanium involved silane monolayers [6, 10, 13, 14], which required several modification steps. In addition, the silane layers may be hydrolyzed under physiological conditions [23]. An ideal, simple and effective immobilization method could be based on a biocompatible and stable linker that can simultaneously bond to titanium and peptides. The purpose of this study was to electrochemically deposit gold nanoparticles onto titanium substrates, followed by the grafting of an RGDC peptide, to improve the biological properties of titanium implants. To the best of our knowledge, few studies on the electrodeposition of Au nanoparticles on titanium surfaces have been reported. Hence, the first step was to evaluate the feasibility of adding nano-structured Au onto titanium surfaces using an electrodeposition method. Secondly, to immobilize RGDC peptides onto nano-Au-deposited titanium surfaces via thiol (–SH) groups was performed. Finally, the effect of the RGDC peptide on the attachment behavior of MG63 cells was examined.

2 Materials and methods

2.1 Electrodeposition of Au nanoparticles

Grade 2 commercially available 1-mm thick titanium plates (99.6 at.%, grade 2, Spemet Co., Taipei, Taiwan) of 10×10 mm^2 were selected as the working electrodes. The plates were mechanically polished with 1,200 grit SiC paper. After that, the substrate surface was ultrasonically cleaned in acetone, 30% HNO_3 and water for 10 min each and then air-dried. The electrodeposition of gold particles was performed in a three-electrode cell connected to a CHI 660A electrochemical system (Austin, TX). Platinum plate and Ag/AgCl were used as the auxiliary and reference electrodes, respectively. The electrochemical deposition of gold nanoparticles was performed in 0.5 M H_2SO_4 solution (J.T. Baker, Phillipburg, NJ) containing 0.5 mM $NaAuCl_4$ (sodium tetrachloroaurate (III) dihydrate, $NaAuCl_4 \cdot 2H_2O$, Sigma, St. Louis, MO) at room temperature by employing a potential step from 0 to −3 V. By varying the deposition time (5, 30, and 60 s), gold nanoparticles with different sizes were deposited onto Ti electrodes. Afterwards, the electrode was removed from the plating cell and washed thoroughly with distilled water and air-dried.

2.2 Morphology and phase composition of Au nanoparticles

Phase and surface morphology of the Ti specimen surfaces following gold electrodeposition were analyzed by TFXRD (Rigaku D/MAX2500, Tokyo, Japan) and SEM (JEOL JSM-6700F, Tokyo, Japan) equipped with an energy dispersive spectrometer (EDS). An atomic force microscope (AFM, NS3a controller with D3100 stage; Digital Instruments, Santa Barbara, CA) was also used to observe the nanostructure of Au particles on the Ti substrate. The AFM system was operated in air by the tapping mode using a silicon cantilever with a sharp tip at its end that was used to scan the specimen surface. The images of 3×3 μm area were obtained with the scan rate of 1 line/s and 512 number of sampling per line.

2.3 Electrochemical measurements of Au nanoparticles

Electrochemical evaluation, including electrochemical impedance spectroscopy (EIS) and cyclic voltammetry (CV) in a conventional three-electrode cell, was performed using an IM6e impedance analyzer (Zahner, Elektrik, Kronach, Germany). A Ag/AgCl plate and a platinum plate were used as the reference electrode and the counter electrode, respectively. Unless otherwise noted, 0.5 M phosphate buffer solution (PBS, pH 7.0) containing 2.5 mM $Fe(CN)_6^{3-/4-}$

(1:1) redox couple (Sigma, St. Louis, MO) was used as the supporting electrolyte in the electrochemical measurements. The CV potential was scanned from −0.6 to +0.5 V at a scan rate of 100 mV/s. In EIS measurements, a 5 mV amplitude sine wave was applied to the electrode at the open circuit potential of 0.4 V in the tested frequency range of 1 Hz to 100 kHz.

2.4 Peptide immobilization and evaluation

For RGDC immobilization, 100 μl of the 0.1, 1 or 10 mM RGDC solution in deionized-distilled water was sprayed onto the coating surfaces for 3 h at room temperature. The specimens were then washed with deionized-distilled water several times and dried at room temperature. The efficacy of peptide grafting was measured by high resolution X-ray photoelectron spectroscopy (XPS, PHI Quantera SXM, ULVAC-PHI, Kanagawa, Japan) equipped with a scanning monochromatized Al X-ray source and 180° spherical capacitor analyzer.

2.5 Cell culture

Cell biocompatibility was evaluated by incubating the specimens with MG63 human osteoblast-like cells (BCRC 60279, Hsinchu, Taiwan). Prior to cell incubation, the specimens were sterilized by soaking in a 75% ethanol solution followed by exposure to ultraviolet (UV) light for 2 h. MG63 cells were suspended in Dulbecco's Modified Eagle's Medium (DMEM, Gibco, Langley, OK) containing 10% fetal bovine serum (Gibco), 1% penicillin (10,000 U/ml)/streptomycin (10,000 mg/ml) solution (Gibco), 0.01 M glycerol-2-phosphate (Sigma, St. Louis, MO), 2.84×10^{-4} M $_{L}$-ascorbic acid (J.T. Baker, Phillipsburg, NJ) and 10^{-10} M dexamethasone (Sigma). MG63 suspensions (1×10^4 cells per well) were directly seeded over each specimen, which was then placed in a 24-well plate. Cell cultures were incubated at 37°C in a 5% CO_2 atmosphere.

2.6 Cell morphology

To observe the cell morphology on the specimen surface, the specimens were washed three times with phosphate-buffered saline (PBS) and fixed in 2% glutaraldehyde (Sigma, St. Louis, MO) for 3 h after 1 and 6 h incubations of the cells. The specimens were then dehydrated using a graded ethanol series for 20 min at each concentration and air-dried at room temperature. The dried specimens were mounted on stubs, coated with gold and inspected using SEM. SEM was operated in the secondary electron image (SEI) mode at an accelerating voltage of 3 kV and magnification of ×1,000.

2.7 Immunostaining

After 1 and 6 h of incubation, cells cultured on the specimens were fixed with 4% paraformaldehyde (Sigma, St. Louis, MO) for 30 min at room temperature and permeabilized with 0.1% Triton X-100 (Sigma, St. Louis, MO) in PBS. Immuno-reaction was carried out by incubating with an antibody to phosphorylated focal adhesion kinase (pFAK, 1:1000, Abcam, Cambridge, UK,) for 2 h followed by three PBS washes. The specimens were then incubated with Alexa Fluor 546-conjugated goat anti-rabbit IgG (Invitrogen, Carlsbad, CA) in PBS for 90 min. Next, the nuclei and actin cytoskeleton were stained for 90 min with 300 nM 4′,6-diamidino-2-phenylindole (DAPI, Invitrogen, Carlsbad, CA) and FITC-conjugated phalloidin (Invitrogen) in PBS, respectively. Immunofluorescence observation was performed using a ZEISS AXioskop2 microscope (Carl Zeiss, Thornwood, NY).

3 Results

3.1 Phase composition

Figure 1 shows the XRD patterns of Ti surfaces before and after 60 s of Au electrodeposition. Three characteristic peaks located at around 35.1°, 38.4°, and 40.1° can be attributed to (100), (002) and (101) crystal faces of Ti (Fig. 1a). A polycrystalline orientation of Au was successfully deposited onto Ti surfaces after electrodeposition (Fig. 1b). A significant number of (111) and (200) crystal faces of Au at 38.4° and 44.4° was detected; the (111) crystal faces overlapped with the Ti (002) plane.

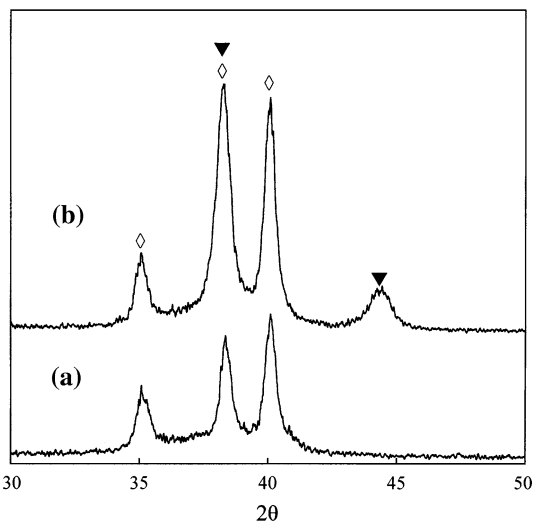

Fig. 1 Thin-film X-ray patterns of Ti substrates (*a*) before and (*b*) after Au nanoparticle electrodeposition for 60 s (◇: Ti; ▼: Au)

3.2 Morphology

In Fig. 2a and b, SEM micrographs show that the size of the Au particles increased with increasing deposition time. A high density of Au nanoparticles could be deposited with a short deposition time (5 s) in a well-dispersed pattern over the titanium surface. As expected, the particle diameter of the Au nanoparticles deposited on the Ti surface increased from around 20 nm after 5 s of deposition to around 50 nm after 60 s of deposition [24]. However, the particle density was not affected by the deposition time. Similarly, the AFM images also show a homogeneous distribution of nano-structured particles (Fig. 2c, d).

3.3 CV

Figure 3 shows the cyclic voltammogram of Ti electrodes with and without Au nanoparticles electrodeposited for different deposition times. On the Ti electrode without Au nanoparticles, the peaks of the reduction of $[Fe(CN)_6]^{3-}$ and oxidation of $[Fe(CN)_6]^{4-}$ disappeared. Furthermore, the Ti electrode without Au nanoparticles exhibited a capacitance response, indicating that there was no electron-transfer reaction. Interestingly, the Au-modified Ti electrodes produced different voltammetric shapes. On the 5-s-deposited Au-modified Ti electrode, a reduction in the peak potential at around −0.4 V was observed. The reduction potential shifted positively toward −0.3 and −0.05 V for the deposition times of 30 and 60 s, respectively.

3.4 EIS

As can be seen in Fig. 4, the complex impedance plot of the Ti electrode without Au nanoparticles exhibited an extremely large semicircular diameter, indicating a high electron-transfer resistance. On the contrary, the semicircular diameter became gradually small with increasing deposition time.

3.5 XPS

RGDC immobilization onto Au-deposited Ti surfaces was examined by investigating the sulfur 2p spectra originating from cysteine containing a thiol (S–H) head group, which can covalently bond to Au. Figure 5 shows the high resolution XPS spectra of the S_{2p} region for 1 mM RGDC peptides immobilized on Ti with and without Au nanoparticles electrodeposited for 60 s. The binding energies of $S_{2p3/2}$ and $S_{2p1/2}$ located on 162.0 and 163.2 eV represented the bound thiolate sulfur atom species (Au–S) and unbound thiol, respectively. It can be clearly seen that the $S_{2p3/2}$ of the RGDC immobilized on an Au-deposited Ti surface had a higher intensity than that obtained from RGDC directly loaded onto a Ti surface.

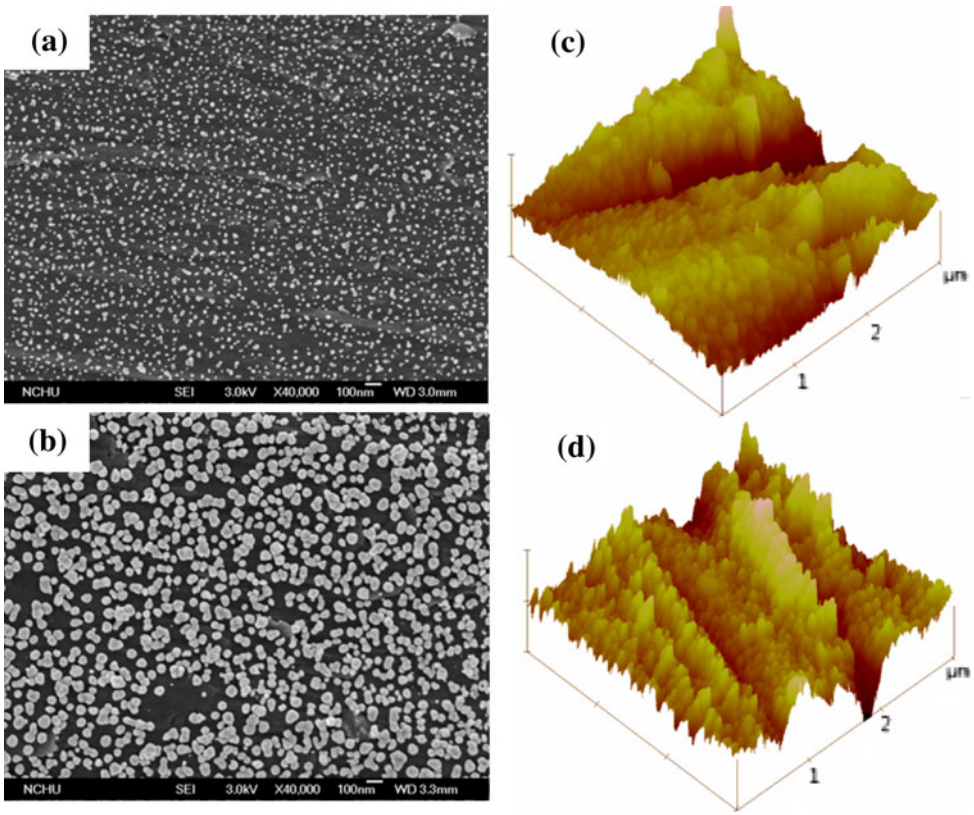

Fig. 2 SEM and AFM images of Au nanoparticles on Ti substrates after different deposition times of (**a**, **c**) 5 and (**b**, **d**) 60 s

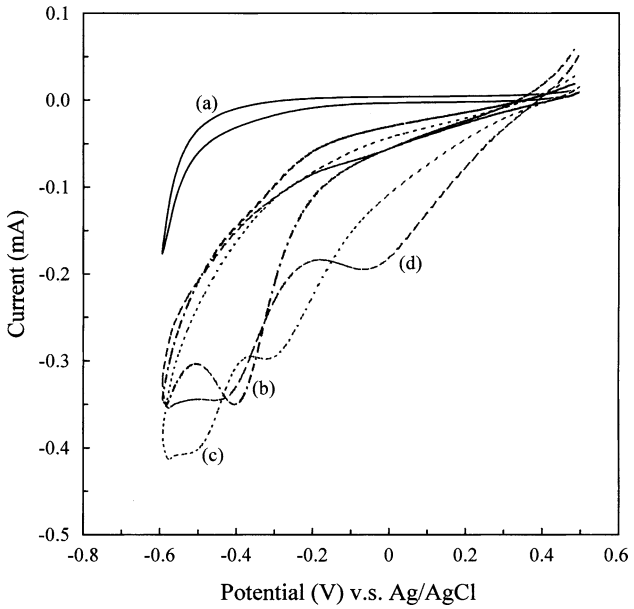

Fig. 3 Cyclic voltammograms of Ti (*a*) before and after Au nanoparticle electrodeposition for (*b*) 5, (*c*) 30 and (*d*) 60 s. The supporting electrolyte was 0.1 M PBS containing 2.5 mM $Fe(CN)_6^{3-/4-}$ redox couple. The scan rate was 100 mV/s in the potential range from −0.6 to +0.5 V

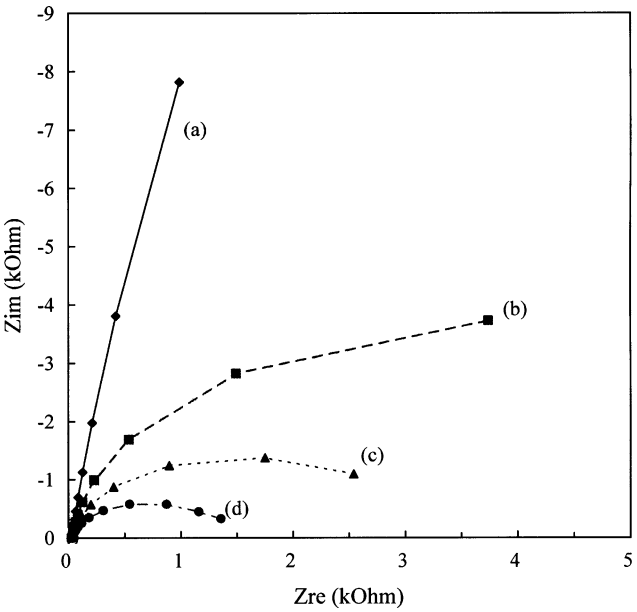

Fig. 4 Nyquist plots (Z_{im} vs. Z_{re}) of Ti (*a*) before and after Au nanoparticle electrodeposition for (*b*) 5, (*c*) 30 and (*d*) 60 s. The supporting electrolyte was 0.1 M PBS containing 2.5 mM $Fe(CN)_6^{3-/4-}$ redox couple. DC voltage: 0.4 V; AC amplitude: 5 mV; frequency range: 1–100 kHz

3.6 Cell morphology

The SEM micrographs of MG63 cells cultured on Ti surfaces with and without Au nanoparticles with different concentrations (0, 0.1, 1 and 10 mM) of RGDC for 1 and 6 h are shown in Fig. 6. In the case of the 1 h incubation, the cells cultured on Ti surfaces without Au nanoparticles had a spherical form, regardless of the RGDC concentration (Fig. 6a). Similar results were observed with cells cultured on Au-deposited Ti surfaces without RGDC immobilization. In contrast, cells cultured on the Ti surfaces with Au deposition and RGDC immobilization demonstrated a more flat morphology (Fig. 6b). After 6 h of culture, some spherical forms of adhered cells could still be observed on Ti surfaces without Au (Fig. 6c). However, cell attachment and spreading became more complete on the RGDC-immobilized Ti with Au nanoparticles and increased with increasing RGDC concentrations (Fig. 6d).

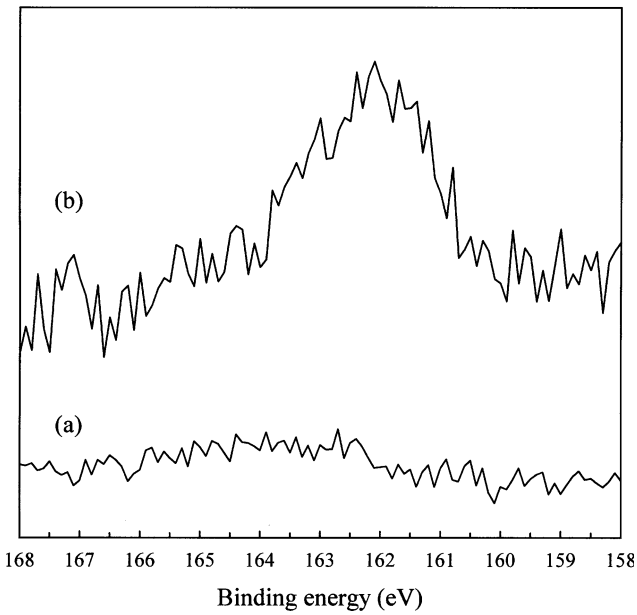

Fig. 5 High resolution XPS S_{2p} spectra for 1 mM RGDC peptide immobilized on Ti (*a*) before and (*b*) after Au nanoparticle electrodeposition for 60 s

3.7 Immunofluorescence observation

In order to further investigate the effect of RGDC on cell functions, pFAK analysis under an immunofluorescence microscopy was employed. Assembly of the actin cytoskeleton was subsequently examined with fluorescent-labeled phalloidin. The immunostaining micrographs are shown in Fig. 7. It can be clearly seen that cells at 1 h of culture on the RGDC-immobilized Ti surfaces with Au demonstrated a higher level of cytoskeletal structure and pFAK compared to those cultured on RGDC directly loaded onto Ti surfaces. In addition, the amount of pFAK increased with increasing RGDC concentration, indicating that the RGD peptide immobilized on Au-deposited Ti binds to the cell-membrane integrins. This binding leads to

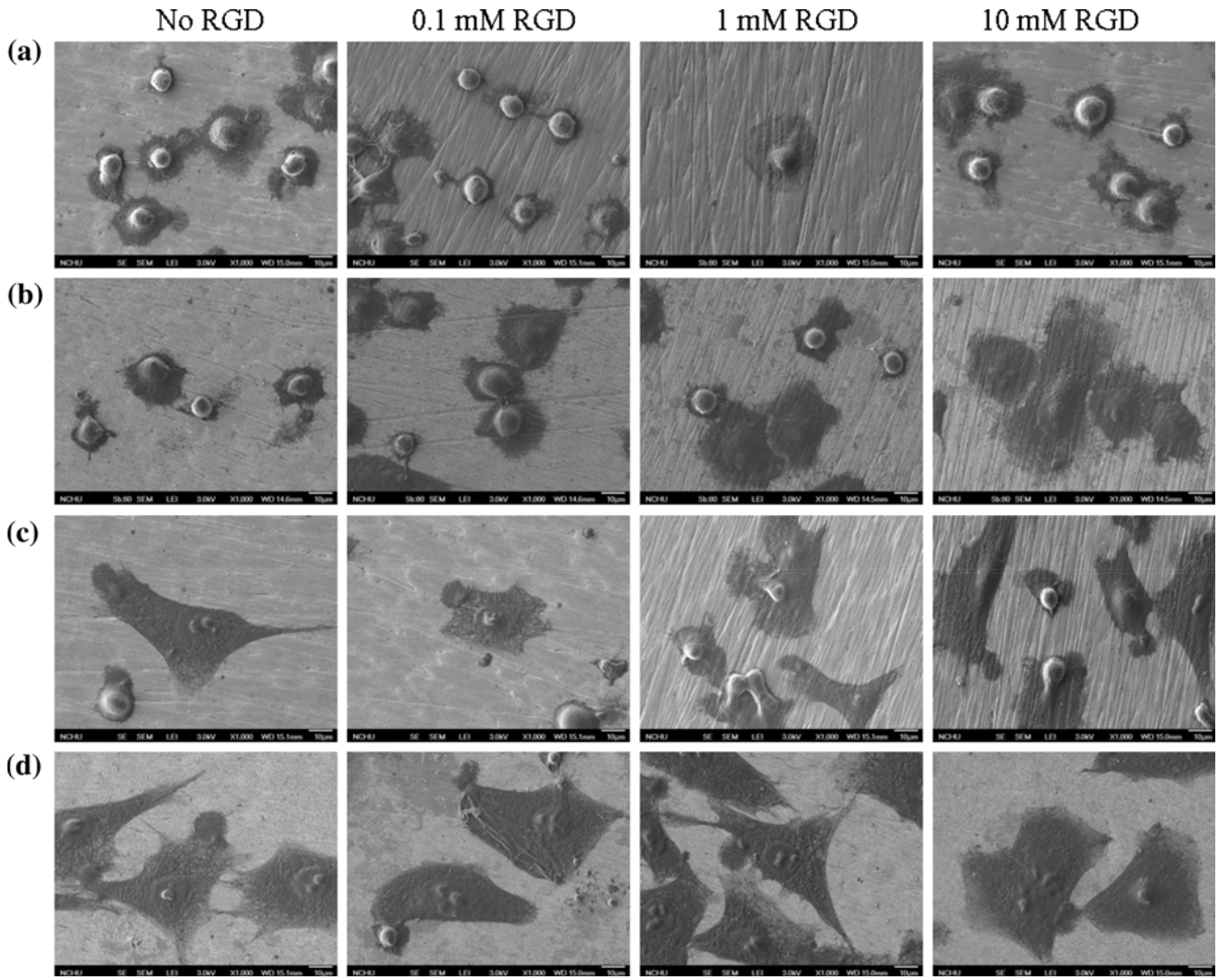

Fig. 6 SEM micrographs of MG-63 cells cultured on different concentrations of RGDC (0, 0.1, 1 and 10 mM) on Ti before (**a**, **c**) and after (**b**, **d**) Au nanoparticles were deposited for 60 s after 1 (**a**, **b**) and 6 h (**c**, **d**) of culture

the formation of focal adhesion and prompts immediate cell adhesion and spreading. Similar to the results of SEM, cells secreted higher amounts of cytoskeletal proteins and pFAK after 6 h of culture. This could be due to the fact that cells had more sufficient time to synthesis extracellular matrix (ECM), thereby enhancing their adhesion and spreading.

4 Discussion

Electrodeposition is a useful method for metal deposition. Nanoscale particles can be easily formed on conducting substrates with relatively short deposition times (Fig. 1), for example, 5 s. In this study, the size of the Au nanoparticles increased with increasing deposition time (Fig. 2). The particles were almost spherical, as reported by EI-Deab [25]. The homogeneity of particle density, irrespective of deposition time, could be attributed to the nucleation properties of Au following the model of instantaneous nucleation, which is a fast process. Thus, the particle density remained constant when the growth and coalescence of deposited particles began [26]. EDS spectra confirmed the presence of Au and Ti without other elements, such as Na and Cl, on the specimen surface. This demonstrates that the Na and Cl ions in the $NaAuCl_4$ solution did not interfere in the formation of the Au nanoparticles.

To check the quality of the Au-modified Ti electrodes, CV and EIS studies were carried out. Generally, in CV curves a couple of well-defined characteristic waves of $Fe(CN)_6^{3-/4-}$ with the peak-to-peak separation (ΔE_p) of about 70 mV can be seen on a bare Au electrode [18]. However, the Ti electrode without Au nanoparticles exhibited a capacitance response (Fig. 3). This can be explained by the fact that a passive oxide film was formed on the Ti surface that suppressed the current flow of the

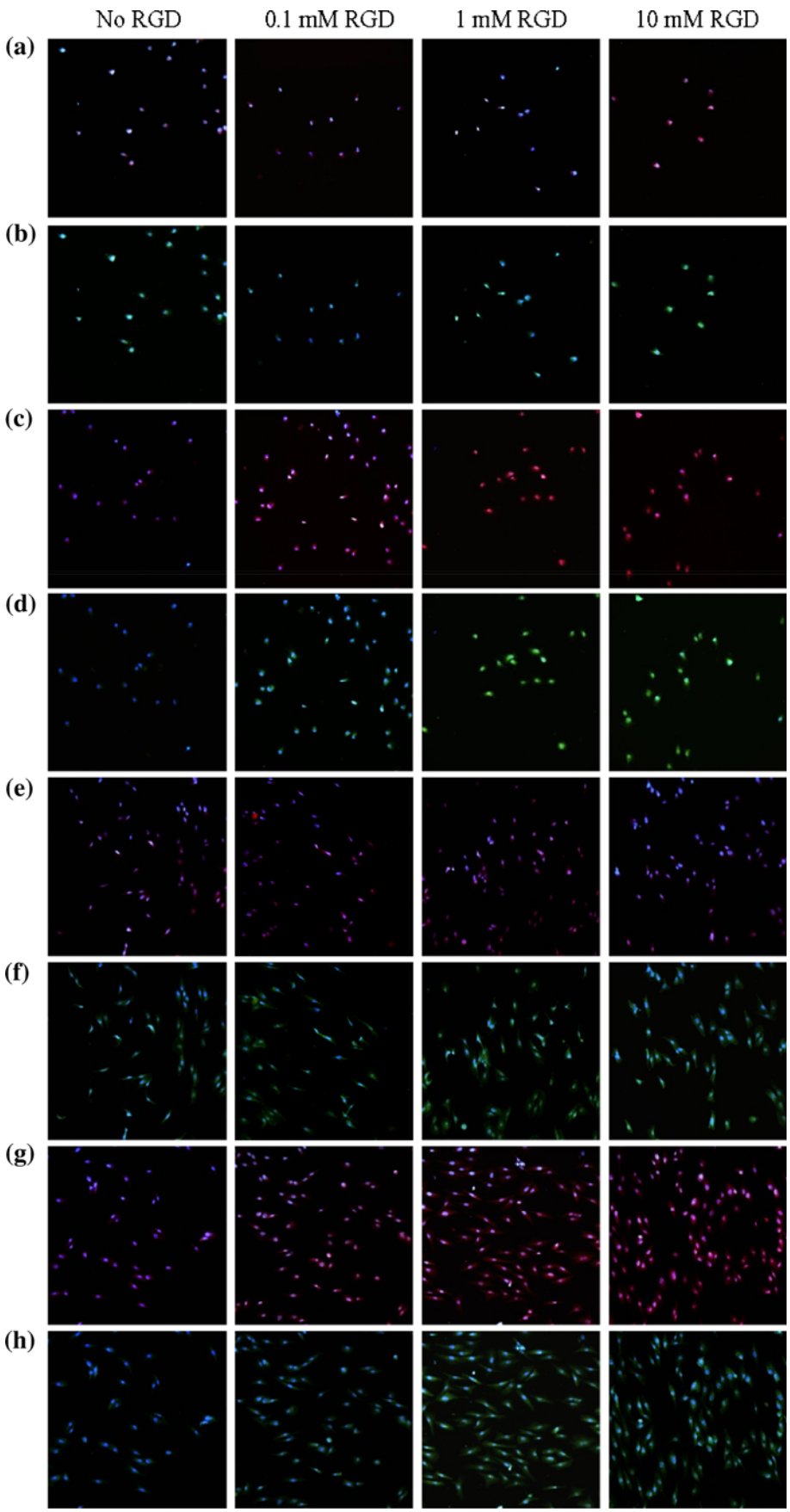

Fig. 7 Immunofluorescence images of MG-63 cells cultured on different concentrations of RGDC (0, 0.1, 1 and 10 mM) on Ti before (**a**, **b**, **e**, **f**) and after (**c**, **d**, **g**, **h**) Au nanoparticles deposited for 60 s after 1 (**a**–**d**) and 6 h (**e**–**h**) of culture. Immunofluorescent staining for nuclei, pFAK, and cytoskeleton proteins. **a**, **c**, **e**, **g** For nuclei and pFAK staining. **b**, **d**, **f**, **h** For nuclei and cytoskeleton staining (magnification: ×200)

$Fe(CN)_6^{3-/4-}$ redox couple. In contrast, two well-separated successive reduction peaks, corresponding to the 2-step, 4-electron reduction of oxygen, took place at 30- and 60-s Au-deposited Ti electrodes [25]. These results reflected an important catalytic feature of the Ti electrode coated with the Au nanoparticles for the reduction of O_2 [27]. It is reasonable that the effective surface area of the Au nanoparticles at the Ti electrode increased with increasing deposition time, as indicated by morphologies, leading to the higher electrocatalytic activity for the 60-s specimens. The results of EIS suggested that the electron-transfer rate was gradually accelerated due to the increasing amount of Au nanoparticles (Fig. 4), consistent with the results of CV. The electrochemical deposition process did form a highly dispersed metal phase with a strongly developed active surface area.

XPS is a highly sensitive surface analysis tool for characterizing the outermost 10 nm of a specimen surface. It can easily define the chemical composition of the specimen surface and can be used to measure the efficacy of peptide grafting. The results of high resolution XPS illustrated that the RGDC peptide could be successfully immobilized on nano-Au-deposited Ti substrates via Au-thiolate species (Fig. 5) [28]. On the contrary, the RGDC peptides on Ti surfaces without Au washed off during the preparation process.

An ideal biomaterial for bone repair and replacement would administer the appropriate signals to direct the processes of osteogenesis, such as cell attachment, proliferation, differentiation, matrix deposition and, ultimately, mineralization of the extracellular matrix. The objective of biological surface modification is to control cell and tissue responses to an implant by immobilizing biomolecules on biomaterials. When the RGD sequence was present on the surface, cellular attachment and spreading took place rapidly with short-term events through the interaction between the RGD sequence and cell-membrane integrins (Fig. 6). These interactions function like physicochemical linkages between the cell and the material [29] and can, in turn, prompt cell proliferation and differentiation in vitro and [16] and in vivo bone formation [17].

Moreover, the recognition and binding of the integrin receptors located on the cell membrane to the RGD sequence on the substrate initiates focal adhesions and subsequently activates FAK by autophosphorylation [30]. FAK, a protein tyrosine kinase, regulates focal contact formation, spreading and induction of signaling pathways that are required for cell motility [31]. Activated FAK and cell attachment were obviously increased on the RGD-modified Ti substrates with Au nanoparticles (Fig. 7), indicating that the modification strategy retained its biological activity and initiated a specific integrin-mediated signal transduction between MG63 cells and the RGDC-modified Ti substrates. In the case of RGD directly loaded onto Ti surfaces without Au nanoparticles, poorer cell attachment and spreading took place, and there was a lower level of FAK. Physical adsorption may not be successful in promoting long-term implantation because of biomolecule desorption [14, 32]. However, the high levels of surface coverage of the peptide, i.e., a higher binding between Ti and RGDC via the Au linker, make this present approach more suitable. Thus, this nano-Au electrodeposition procedure could be used as an alternative method for biomolecule immobilization.

5 Conclusions

The Au nanoparticles with polycrystalline orientation were well dispersed on the titanium surface and had a uniform particle size of about 50 nm after electrodeposition for 60 s. The particle size of the nano-structured Au was dependent on the deposition time. No redox reaction of $Fe(CN)_6^{3-/4-}$ was observed on the titanium substrate, possibly due to the blocking effect of the naturally formed titanium oxide. The EIS measurement indicated that the nano-gold decreased the electron-transfer resistance. The RGDC peptide could be immobilized on Au nanoparticle-deposited Ti substrates via the covalent Au–S bonding. Cell morphology and results of the pFAK assay consistently demonstrated that the arrays of electrodeposited gold nanoparticles on titanium substrates provide an effective tool to subtly control RGDC immobilization with greater stability.

Acknowledgments The authors acknowledge the financial support of Changhua Christian Hospital and Chung Shan Medical University under the contract No. 97-CCH-CSMU-08.

References

1. Noort VR. Titanium: the implant material of today. J Mater Sci. 1987;22:3801–11.
2. Carlsson L, Röstlund T, Albrektsson B, Albrektsson T, Brånemark P. Osseointegration of titanium implants. Acta Orthop Scand. 1986;57:285–9.
3. Ding SJ. Surface modification of implant metals for hard tissue replacements. In: Tanaka J, Itoh S, Chen G, editors. Surface design and modification of biomaterials for clinical application, Chapter 2. Research Signpost, Kerala, India; 2008. pp. 29–59.
4. Ding SJ, Ju CP, Chern Lin JH. Characterization of hydroxyapatite and titanium coatings sputtered on Ti-6Al-4V substrate. J Biomed Mater Res. 1999;44:266–79.
5. Chen CC, Huang TH, Kao CT, Ding SJ. Characterization of functionally graded hydroxyapatite/titanium composite coatings plasma-sprayed on Ti alloys. J Biomed Mater Res. 2006;78B:146–52.
6. Matinlinna JP, Laajalehto K, Laiho T, Kangasniemi I, Lassila LVJ, Vallittu PK. Surface analysis of Co-Cr-Mo alloy and Ti substrates silanized with trialkoxysilanes and silane mixtures. Surf Interface Anal. 2004;36:246–53.

7. Nagai M, Hayakawa T, Fukatsu A, Yamamoto M, Fukumoto M, Nagahama F, et al. In vitro study of collagen coating of titanium implants for initial cell attachment. Dent Mater J. 2002;21: 250–60.
8. Abe Y, Hiasa K, Takeuchi M, Yoshida Y, Suzuki K, Akagawa Y. New surface modification of titanium implant with phosphoamino acid. Dent Mater J. 2005;24:536–40.
9. Keselowsky BG, Collard DM, García AJ. Surface chemistry modulates fibronectin conformation and directs integrin binding and specificity to control cell adhesion. J Biomed Mater Res. 2003;66A:247–59.
10. Nanci A, Wuest JD, Peru L, Brunet P, Sharma V, Zalzal S, et al. Chemical modification of titanium surfaces for covalent attachment of biological molecules. J Biomed Mater Res. 1998;40: 324–35.
11. Zorn G, Gotman I, Gutmanas EY, Adadi R, Sukenik CN. Surface modification of Ti45Nb alloy by immobilization of RGD peptide via self assembled monolayer. J Mater Sci Mater Med. 2007;18: 1309–15.
12. Adden N, Gamble LJ, Castner DG, Hoffmann A, Gross G, Menzel H. Phosphonic acid monolayers for binding of bioactive molecules to titanium surfaces. Langmuir. 2006;22:8197–204.
13. Xiao SJ, Textor M, Spencer ND. Covalent attachment of cell-adhesive (Arg-Gly-Asp)-containing peptides to titanium surfaces. Langmuir. 1998;14:5507–16.
14. Porté-Durrieu MC, Guillemota F, Pallu S, Labrugère C, Brouillaud B, Bareille R, et al. Cyclo-(DfKRG) peptide grafting onto Ti-6Al-4V: physical characterization and interest towards human osteoprogenitor cells adhesion. Biomaterials. 2004;25:4837–46.
15. Dettin M, Bagno A, Gambaretto R, Iucci G, Conconi MT, Tuccitto N, et al. Covalent surface modification of titanium oxide with different adhesive peptides: surface characterization and osteoblast-like cell adhesion. J Biomed Mater Res. 2009;90A:35–45.
16. Kantlehner M, Schaffner P, Finsinger D, Meyer J, Jonczyk A, Diefenbach B, et al. Surface coating with cyclic RGD peptides stimulates osteoblast adhesion and proliferation as well as bone formation. Chembiochem. 2000;1:107–14.
17. Schliephake H, Scharnweber D, Dard M, Rossler S, Sewing A, Meyer J, et al. Effect of RGD peptide coating of titanium implants on periimplant bone formation in the alveolar crest. An experimental pilot study in dogs. Clin Oral Implants Res. 2002;13:312–9.
18. Ding SJ, Chang BW, Wu CC, Lai MF, Chang HC. Electrochemical evaluation of avidin-biotin interaction on self-assembled gold electrodes. Electrochim Acta. 2005;50:3660–6.
19. Baschong W, Stiethof YD. Preparation, use, and enlargement of ultrasmall gold particles in immunoelectron microscopy. Microsc Res Tech. 1998;42:66–79.
20. Yan W, Chen B, Mahurin SM, Schwartz V, Mullins DR, Lupini AR, et al. Preparation and comparison of supported gold nanocatalysts on anatase, brookite, rutile, and P25 polymorphs of TiO_2 for catalytic oxidation of CO. J Phys Chem B. 2005;109:10676–85.
21. Finot MO, Braybrook GD, McDermott MT. Characterization of electrochemically deposited gold nanocrystals on glassy carbon electrodes. J Electroanal Chem. 1999;466:234–41.
22. Li CZ, Liu Y, Luong JHT. Impedance sensing of DNA binding drugs using gold substrates modified with gold nanoparticles. Anal Chem. 2005;77:478–85.
23. Puelo D. A. Retention of enzymatic activity immobilized on silanized Co-Cr-Mo and Ti-6Al-4V. J Biomed Mater Res. 1997;37: 222–8.
24. Olson TS, Atanassov P, Brevnov DA. Electrodeposition of gold particles on aluminum substrates containing copper. J Phys Chem B. 2005;109:1243–50.
25. El-Deab MS, Ohsaka T. An extraordinary electrocatalytic reduction of oxygen on gold nanoparticles-electrodeposited gold electrodes. Electrochem Commun. 2002;4:288–92.
26. Penner RM. Mesoscopic metal particles and wires by electrodeposition. J Phys Chem B. 2002;106:3339–53.
27. Zhang JD, Kambayashi M, Oyama M. Seed mediated growth of gold nanoparticles on indium tin oxide electrodes: electrochemical characterization and evaluation. Electroanalysis. 2005;17: 408–16.
28. Castner DG. X-ray photoelectron spectroscopy sulfur 2p study of organic thiol and disulfide binding interactions with gold surfaces. Langmuir. 1996;12:5083–6.
29. Siebers MC, ter Brugge PJ, Walboomers XF, Jansen JA. Integrins as linker proteins between osteoblasts and bone replacing materials. A critical review. Biomaterials. 2005;26:137–46.
30. Abbi S, Guan JL. Focal adhesion kinase: protein interactions and cellular functions. Histol Histopathol. 2002;17:1163–71.
31. Cohen-Hillel E, Yron I, Meshel T, Soria G, Attal H, Ben-Baruch A. CXCL8-induced FAK phosphorylation via CXCR1 and CXCR2: cytoskeleton- and integrin-related mechanisms converge with FAK regulatory pathways in a receptor-specific manner. Cytokine. 2006;33:1–16.
32. Castner DG, Ratner BD. Biomedical surface science: foundations to frontiers. Surf Sci. 2002;500:28–60.